JOURNAL OF COMPUTATIONAL PHYSICS 101, 140–150 (1992)

The Atomic Strain Tensor

PETER H. MOTT

Department of Materials Science and Engineering, Massachusetts Institute of Technology, Cambridge, Massachusetts

ALI S. ARGON

Department of Mechanical Engineering, Massachusetts Institute of Technology, Cambridge, Massachusetts

AND

ULRICH W. SUTER

Institut für Polymere, Eidgenössische Technische Hochschule, Zürich, Switzerland and
Department of Chemical Engineering, Massachusetts Institute of Technology, Cambridge, Massachusetts

Received October 19, 1990; revised June 20, 1991

A definition of the local atomic strain increments in three dimensions and an algorithm for computing them is presented. An arbitrary arrangement of atoms is tessellated into Delaunay tetrahedra, identifying interstices, and Voronoi polyhedra, identifying atomic domains. The deformation gradient increment tensor for interstitial space is obtained from the displacement increments of the corner atoms of Delaunay tetrahedra. The atomic site strain increment tensor is then obtained by finding the intersection of the Delaunay tetrahedra with the Voronoi polyhedra, accumulating the individual deformation gradient contributions of the intersected Delaunay tetrahedra into the Voronoi polyhedra. An example application is discussed, showing how the atomic strain clarifies the relative local atomic movement for a polymeric glass treated at the atomic level.

1. INTRODUCTION

Computer modelling provides coordinates of all atoms of model systems at any time. One fundamental property of interest is how the local atomic structure changes in response to a globally applied "driving force," for example, a stress or strain increment. Scrutinizing atomic displacements has been the usual method to study how local structure changes, but this method does not lend itself to structurally meaningful conclusions, especially in three-dimensional systems. Atomic displacements show the distance and direction of movement for each atom, but gives no information on the change in position of an atom with respect to its neighbors. To study the motion of atoms in response to an applied driving force in a meaningful way, we must define an "atomic strain tensor."

The algorithm presented below is best suited for the deformation of a dense, disordered system with periodic boundaries, such as a glass. Deng *et al.* [1] published a study on a two-dimensional system and used the notion of atomic strain, but the method employed cannot be extended to analyzing the topology of three-dimensional assemblies. Many other workers, such as Clarke and Brown [2], Maeda and Takeuchi [3], and Srolovitz *et al.* [4], have studied atomic displacements in three-dimensional glasses, without using atomic strain as a means to isolate regions of high atom mobility. As far as we know, atomic strain has not been defined for three-dimensional systems nor has an algorithm that calculates atomic strain been developed for such systems.

In Section 2, we briefly review two alternative and complementary ways of tessellating space, as a means to define and clarify the terms used in later sections. We define the "atomic strain" in Section 3. Section 4 explores the topological details further in order to implement atomic strain. In Section 5, we outline the algorithm explicitly. Finally, Section 6 sketches out an example application of the program to the deformation of a polymeric glass, the details of which will be published elsewhere.

2. TESSELLATION OF SPACE

The atomic strain requires a precise way to divide the volume allotted to an atom and an unambiguous way to identify the interstices in a system. The Voronoi and Delaunay tessellations are methods that meet this requirement. Our development builds on the work of Tanemura *et al.* [5].

Let a set of distinct points ("atoms") be distributed in a parallelepiped ("box") of some finite size. Assume that the

0021-9991/92 $5.00

entirety of three-dimensional space is covered by replicas of this box. The region in space closest to a given atom defines the Voronoi polyhedron enclosing the atom. These polyhedra are convex figures that are bounded by planar faces. A "face plane" between two atoms is obtained by drawing a line segment connecting the two atoms, and then constructing a plane that is the perpendicular bisector to the line segment. Any point that lies on this face plane is equidistant to the two atoms. Where two face planes meet defines an edge, and where three face planes meet forms a corner. Thus, the "face" is a region of the face plane that is bounded by the edges formed by the intersections with other face planes. The existence of a common face is the criterion used to determine "neighboring atoms." The set of polyhedra constructed around all atoms fills space in the box without any gaps or overlaps.

Joining all neighboring atoms by straight lines produces a space network. The set of four atoms that are neighbors to each other forms a tetrahedron. The set of tetrahedra for a given set of atoms also tessellates space and is called the Delaunay tessellation. We term the elementary tetrahedron in this tessellation the Delaunay tetrahedron and abbreviate it DT. The tetrahedra also have planar faces, edges, and corners: the face of a DT is a part of a plane defined by the positions of three atoms, bounded by the edges formed by line segments joining the atoms; the corners are the positions of the atoms. "Neighboring DTs" are defined to be any two DTs that share a face. The set of DTs that all contain a given atom is a closed figure around that atom, not necessarily convex.

Any four points that do not lie on a plane define a sphere, and if a sphere is constructed that passes through the vertex atoms of a Delaunay tetrahedron, the center of the sphere is equidistant to the four atoms. Thus, the center defines a corner shared by the four Voronoi polyhedra containing the corner atoms. The center of the sphere need not lie inside the tetrahedron. The two tessellations, Voronoi and Delaunay, are dual to each other: the Voronoi tessellation describes space that "belongs" to the atoms, while the Delaunay tessellation describes the interstitial regions that are bounded by four atoms. Both tessellations are unique for a given set of atoms. The algorithm used for both tessellations is essentially that of Tanemura *et al.* [5], modified to handle an arbitrary, non-orthogonal periodic parallelepiped.

3. ATOMIC STRAIN

In the macroscopic, continuum sense, a strain increment is defined by the change in length and orientation of an infinitesimal line segment and is a function of position in the body. On the atomic level, only the change in the relative position of the neighboring atoms is unambiguously definable, and in interstitial regions, the strain must be regarded as constant. Because the tetrahedra found by the Delaunay tessellation are necessarily empty of any other atoms, they provide a convenient geometrical basis on which to define strain increments on the atomistic scale.

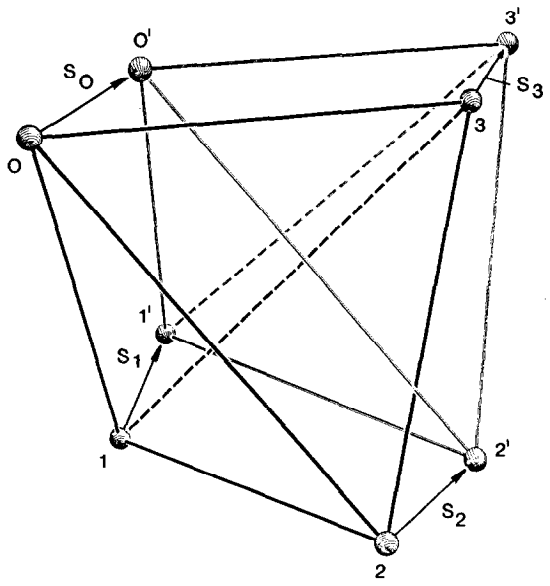

FIG. 1. Displacement and distortion of a Delaunay tetrahedron.

Consider such an interstitial region between the atoms in a Delaunay tetrahedron shown in Fig. 1, where the atoms have experienced an increment of movement. Take atom 0 to be the atom of interest and place its original position at the origin. The displacement of each atom is $\mathbf{s}_i$, where i is the atom number. The relative displacement $\mathbf{u}_i$ of atom i is then $\mathbf{s}_i - \mathbf{s}_0$. We define the deformation gradient tensor $\mathbf{F}$ inside a tetrahedron by differentiating the relative displacements $\mathbf{u}$ of the four corner atoms of the tetrahedron, with respect to the three directions of the Cartesian coordinate system, $\mathbf{x}$:

$$\mathbf{F} = \frac{\partial \mathbf{u}}{\partial \mathbf{x}}. \tag{1}$$

The relative motion of the atoms of the DT can provide no further information regarding higher order derivatives of displacement, and so the displacement gradient inside the tetrahedron has been assumed to be constant. The displacement field $\mathbf{u}$ so defined is piecewise continuous along the faces and edges of each DT.

The displacement gradient defined in Eq. (1) is conservative and correct, but is associated with interstitial space, not with atoms. An atom belongs typically to 20–30 DTs, each with a different shape, volume, and displacement gradient; we are interested in the resulting strain increments associated with atoms, not with interstices. Thus, the information in Eq. (1) needs to be re-allocated proportionally according to the volume belonging to the atoms. Therefore, to find the deformation gradient of an atom, it is necessary

to identify all the DTs sampled by the Voronoi polyhedron constructed around the atom. Symbolically, we find the deformation gradient $\mathbf{F}_i$ for atom i by the weighted sum over all DTs that the Voronoi polyhedron intersects; i.e.,

$$\mathbf{F}_i = \sum_j^{\text{DTs}} k_{ij}\mathbf{F}_j, \tag{2}$$

where k_{ij} is the volume fraction of the Voronoi polyhedron that falls inside the jth DT. By using the initial position of the atom i as the origin, we have used an infinitesimal Lagrangian representation to find deformation gradients $\mathbf{F}_j$ of the DTs. To be consistent with this, the intersecting volume fraction k_{ij} needs to be evaluated from the initial positions of the atoms. The atomic strain increment tensor $\boldsymbol{\varepsilon}_i$ for atom i is then found from the atomic deformation gradient $\mathbf{F}_i$ by subtracting out the rigid-body rotations in the usual way. Of this strain tensor, two scalar invariants are of special interest, the local dilatation ε, and the local deviatoric distortion γ, which are defined as:

$$\varepsilon = \operatorname{Tr} \boldsymbol{\varepsilon} \tag{3}$$

$$\gamma^2 = \tfrac{2}{3}\operatorname{Tr}(\boldsymbol{\varepsilon} - \tfrac{1}{3}\varepsilon\mathbf{I})^2. \tag{4}$$

4. THE APPROACH TO THE PROBLEM

We address the problem using the original structure as the "ground state," and the strained structure is compared to the original. The intersecting volume fraction k_{ij} is found from the ground state, so that the detailed Voronoi and Delaunay constructions for the original structure are needed as input. The information required is the atom neighbor list for each atom, the volume of the Voronoi polyhedra, and the set of Delaunay tetrahedra. The number of atoms in the original structure must equal the number of atoms in the strained structure.

Throughout the procedure, there are many places where conservation laws are used to ensure that an operation is done correctly. The most sensitive is that the volume weighted sum of the local atomic level strains must exactly equal the imposed strain on the whole system. It has been found that if a single DT is changed or omitted from the inputted DT set (in the test data sets, there were about 3100 DTs), the summation of the atomic deformation gradients deviates from the system gradient by about 1%. This is a large, obvious error, compared to the computer working precision of about 10^{-15}; the strain program outlined here is quite sensitive to any errors in tessellating the system.

There are two parts to find the atomic displacement gradient, calculating $\mathbf{F}$ for each DT and finding the intersections k_{ij}. Finding the deformation gradient for each DT is straightforward, and this is calculated at the beginning of the program. The major effort in the algorithm is to find the intersections of all DTs with a single Voronoi polyhedron. We call the atom that the Voronoi polyhedron is formed around the "central atom." This procedure is repeated for all atoms in the system.

If a DT intersects a Voronoi polyhedron, it is apparent that the DT must enter the Voronoi polyhedron at one or more Voronoi face(s). Consider the intersection of a DT with a plane, shown in Fig. 2. A DT can intersect the plane only when the corners of the tetrahedron lie on both sides of the plane. The two possibilities are: two atoms on each side, or one atom on one side and three atoms on the other. The illustration shows that the intersection must be either a three- or four-sided polygon. Because the set of DTs tessellates space, the intersection of DTs with any plane must tessellate the plane. We do not consider the degenerate case when an atom sits exactly on the plane; rather, if an atom does happen to lie on the plane, we shall assume that it lies on the positive side, as defined by the direction of the plane normal. The error introduced by this simplification is within the machine working precision.

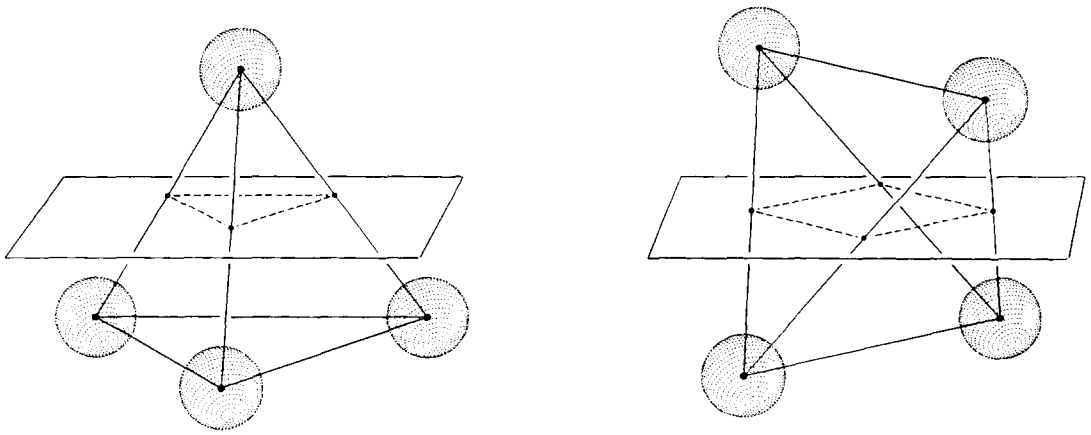

FIG. 2. The intersection of a tetrahedron with a plane.

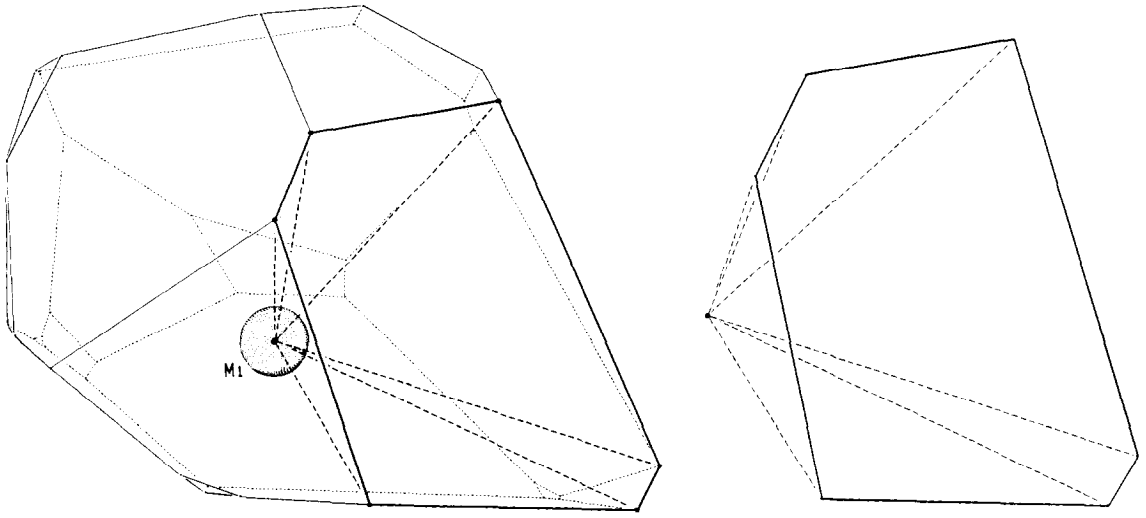

FIG. 3. Voronoi polyhedron around atom $M1$. A pyramidal figure formed by connecting a face (shown in bold) to the central atom has been cut out on the right.

Since an intersecting DT must penetrate a Voronoi polyhedron at a face, it is natural to further divide the polyhedron into composite pyramidal figures—one pyramid for each face of the polyhedron. The base plane of the pyramid is then the Voronoi face, and the "peak" of the pyramid is the position of the central atom. Figure 3 shows the Voronoi polyhedron surrounding atom $M1$ with such a composite pyramid cut out for closer inspection. Triangular side faces of the pyramid are formed by joining the edges of the face to the apex. Two such pyramids inside a Voronoi polyhedron that have a common edge share a side face. It is evident that the pyramids so constructed completely cover the volume without overlap inside any given Voronoi polyhedron.

In Fig. 4 the face that was cut out in Fig. 3 is shown in greater detail. The two atoms that share the face are shown, atom $M1$ is below, behind the face plane, and atom $H3$ is above the plane. Note that the face does not intersect the line segment connecting the two atoms; this was found to be a frequent occurrence. The corners of the face are labeled

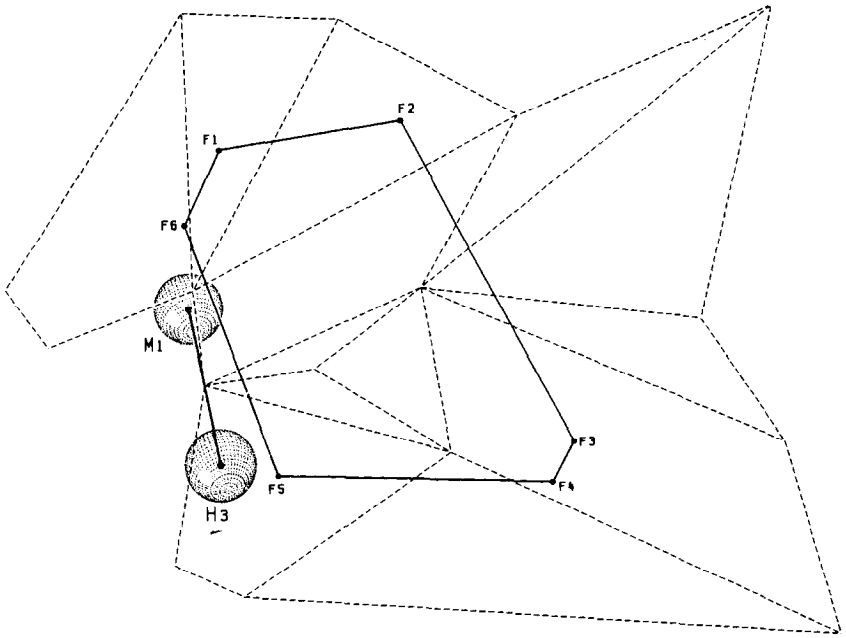

FIG. 4. Detail of the face cut out in Fig. 3. The points $F1, \ldots, F6$ are the corners of the face, and the bold lines between the corners are the edges. The face is shared by Voronoi polyhedra formed around atoms $M1$ and $H3$. The atom $M1$ is behind the plane, atom $H3$ is in front. The dashed lines all lie in the face plane, indicating where various contributing DTs intersect the Voronoi face.

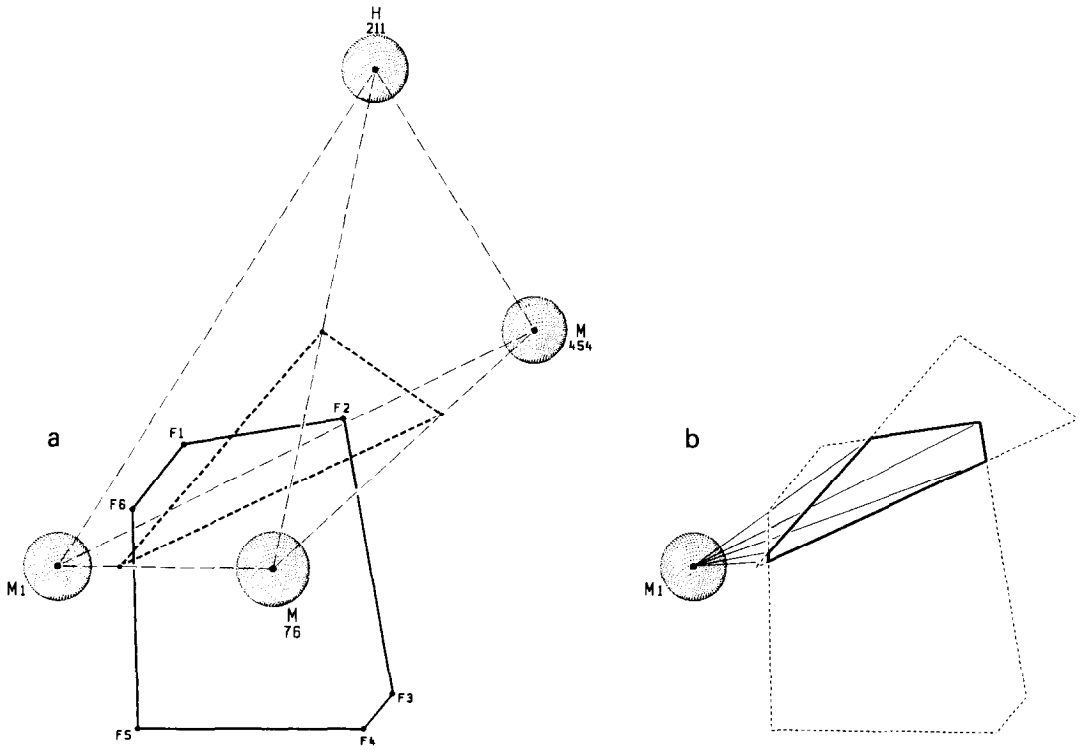

FIG. 5. (a) The intersection of a DT with the Voronoi face shown in Fig. 3 and 4. The atoms $M1$, $H211$, $M454$ lie behind the plane, and atom $M76$ is in front of the plane. (b) The "subpyramid" formed by the intersecting face-DT area, shown in bold.

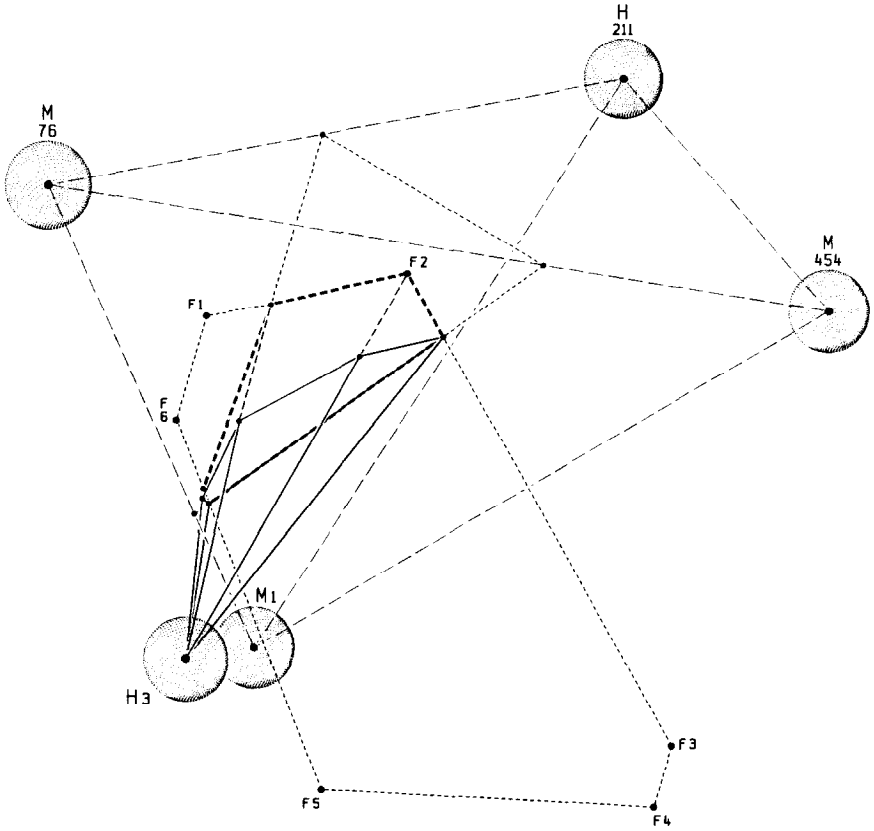

FIG. 6. The subpyramid using the same intersection between the DT and the face seen in Fig. 4, but using the atom $H3$ as the central atom peak, instead of atom $M1$. The atoms $M1$, $H211$, and $M454$ lie behind the plane, and atoms $H3$ and $M76$ are in front. The face has been rotated slightly from Fig. 4.

$F1, ..., F6$. The tessellating three- and four-sided figures formed by the dashed lines all lie in the face plane and are the intersections of DTs that have some part falling inside the face, which will make a contribution to the strain of atom $M1$.

The composite pyramid that was formed from a Voronoi face may be further divided into more elementary "subpyramids," using the areas of the dashed DT intersections that lie within the face as the bases. For example, Fig. 5a focuses on the DT intersecting the face that contains the corner $F2$ of the same face seen in Figs. 3 and 4. We take atom $M1$ to be the central atom; for clarity the neighboring atom $H3$ has been omitted. The DT that intersects with the face is made up of atoms $\{M1, M76, H211, M454\}$, shown as light dashed lines. Atoms $M1$, $H211$, and $M454$ lie below, behind the face plane, while atom $M76$ is above the plane. The DT intersection with the face plane is shown as a heavy dashed line. The base of the subpyramid formed by the intersection area is shown by the bold line in Fig. 5b. The subpyramid is precisely the intersection of the DT with the Voronoi face pyramid.

Supposing now that the central atom is not atom $M1$, as assumed in Fig. 5, but the other, neighboring atom $H3$ (see Fig. 4). This situation is illustrated in Fig. 6, focusing now on the same face shown in Fig. 3, 4, and 5, but with some enlargement and a slight rotation. The pyramids formed on either side of the face are mirror images, so their volumes must be equal. Atom $M1$ is still below, behind the face plane, and atom $H3$ is above. The same intersecting DT $\{M1, M76, H211, M454\}$ is shown as in Fig. 5a, where $H211$ and $M454$ are behind the plane, and $M76$ is above, in front of the plane. The central atom $H3$ is *not* a member of this intersecting DT. The heavy dashed lines in Fig. 6 form the subpyramid base, as shown in Fig. 5b; the two subpyramids in Figs. 5b and 6 are mirror images, so again, their volumes must be equal. Starting at the base of the subpyramid and following it to the peak at the central atom $H3$, the subpyramid emerges from the DT that contains the base, into a neighboring DT: the DT face formed by the atoms $\{M1, M76, M454\}$ is where the subpyramid emerges. The edges of the subpyramid are drawn with medium dashed lines behind this "exiting" face, inside the DT that contains the base; outside the DT, in front of the exiting DT face, the subpyramid edges are drawn with solid lines. The intersection of the DT face $\{M1, M76, M454\}$ and the subpyramid is also shown with solid lines. The part of the subpyramid inside the DT that contains the base (drawn with dashed lines) is the intersection of the DT $\{M1, M76, H211, M454\}$ with the Voronoi face pyramid. The remaining part of the subpyramid forms a new, smaller sub-subpyramid, with its base on the exiting DT face plane.

The subpyramid illustrated in Fig. 6 enters a new DT that does not contain the base. This must be so for every DT that does not contain the central atom but does intersect the Voronoi face, because the set of DTs that all contain a given atom form a closed figure about that atom. The intersection of a DT with a Voronoi face that does not contain the central atom indicates an "obtuse" Voronoi polyhedron, a polyhedron that extends beyond the enclosing figure formed from the DTs. A two-dimensional analogy is shown in Fig. 7. Obtuse Voronoi polyhedra were found to be much more common in three-dimensional systems than in two-dimensional systems. Returning to the sub-subpyramid defined in Fig. 6, starting at the base and following it to the central atom peak, it is necessary to identify the neighboring DT that contains the new base. Supposing that this neighboring DT also does not contain the central atom $H3$, the sub-subpyramid must emerge from this DT as well, and another subpyramid piece like the one seen inside the DT in Fig. 6 will be constructed. This will spawn yet another sub-sub-subpyramid. This procedure is repeated until the subpyramid finally enters a DT that contains the central atom. This DT will contain the apex, and thus there will be no more "exits."

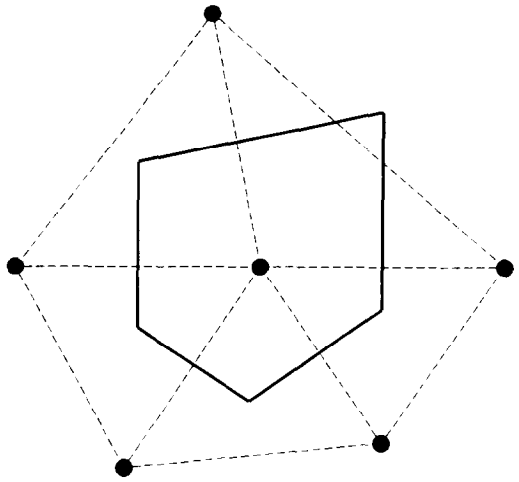

FIG. 7. Two-dimensional example of an obtuse Voronoi polygon. The atoms are the filled circles, the dashed lines are Delaunay triangles, and the enclosing Voronoi polygon is shown by the heavy solid line.

5. ALGORITHM

I. Initialization. Input $\{A\}$, the positions of the set of atoms; $\{N\}$, the neighbor list for each atom; $\{Q\}$, the volume fractions of the Voronoi polyhedra; and $\{T\}$, the set of DTs for the "original" structure. Input $\{B\}$, the positions of the atoms for the "strained" structure.

A. For each tetrahedron T_j in $\{T\}$, find:

1. The position of the center of the sphere C_j that passes through the atoms A_i, $A_i \in T_j$, which corresponds to a corner of a Voronoi polyhedron.

2. The volume fraction of the tetrahedron ϕ_j, and the displacement gradient $\mathbf{F}_j$. Finding the displacement gradients is the only point in the program where the "strained" atom positions $\{B\}$ are used.

B. Check that $\sum \phi_j = 1$ and $\sum \phi_j \mathbf{F}_j = \mathbf{F}_{\text{system}}$.

C. For each T_j in $\{T\}$, find the DT that contains the circumcenter C_j that belongs to T_j. Denote this set $\{\Theta(C)\}$.

II. Main part of algorithm. For each atom A_i in $\{A\}$:

A. Obtain the set of Voronoi face planes $\{P\}$, constructed from the neighbor list $\{N\}$.

B. Define the set $\{K\}$ to be the "master" list of DTs sampled by the Voronoi polyhedron about atom A_i. For each DT K_m in $\{K\}$, define the variable k_{im}, the volume fraction of K_m intersected by the Voronoi polyhedron about atom A_i. Initially, the set $\{K\}$ is empty and $\{k_i\}$ is set to zero.

C. For each Voronoi face plane P_k in $\{P\}$:

1. Obtain the set of corners $\{c\}$ of the face, $\{c\}$ is a subset of $\{C\}$, and the set of DTs $\{\theta(c)\}$ that contain these corners, $\{\theta(c)\}$ is a subset of $\{\Theta(C)\}$. The corners must be ordered around the face along a single closed path. Start the list of DTs sampled by the Voronoi polyhedron face $\{S\}$ by setting $\{\theta(c)\} \rightarrow \{S\}$.
2. Obtain the area of the face a_k and the volume fraction of the pyramid Ω_k formed, using the face as the base and the central atom as the peak.
3. Form the edges between the corners by connecting the points c_n and c_{n+1}. Starting with the DT that contains c_n, $\theta(c_n)$, detect the DT face where the edge "exits." Find the neighboring DT to this exit-face. Repeat this procedure until the line segment arrives in the DT that contains the corner c_{n+1}, θ_{n+1}. In this fashion, circle around the edge of the face, detecting all DTs that intersect with the face edge. Add any newly detected DTs to the set $\{S\}$.
4. Consider a set of atom pairs $\{A_q, A_r\}$ that represents a DT edge, where A_q and A_r are on opposite sides of the face plane P_k. Form the set of DT edges, $\{e\}$, from the intersecting DT set $\{S\}$, such that the intersection of the edge to the face plane F_k falls *inside* the face. Next, from $\{T\}$, obtain the set of DTs $\{E\}$ that contain the atom pairs found in $\{e\}$, i.e., all DTs that share the DT edges that fall inside the Voronoi face. Add any DTs in $\{E\}$ not in $\{S\}$ to the set $\{S\}$. This completes the set $\{S\}$. This completes the set $\{S\}$, the DTs that intersect the face P_k, seen as dashed lines in Fig. 4.
5. For each DT S_m in $\{S\}$, find the area δ_m of the face contained by the DT intersection. This corresponds to the area traced out by the bold line in Fig. 5b. Check that the area is conserved, that is, $\sum \delta_m = a_k$.
6. It is possible that all the corners in $\{c\}$ lie inside a single DT, in which case the set $\{\theta(c)\}$ has only one distinct DT and the set $\{S\}$ has only one element. In this case, the Voronoi face edge will never cross into another DT, and the entire face is completely contained by the DT in $\{\theta(c)\}$. Here, the face area a_k is equal to the intersecting DT area δ.
7. For each DT S_m in $\{S\}$, find the volume fraction of the subpyramid w_m that has the intersecting area δ_m as the base and the central atom i as the summit, as shown in Fig. 5b.
8. Form a new set $\{\pi\}$ by setting $\{S\} \rightarrow \{\pi\}$. This will be the set of DTs that intersect the pyramid formed from the face P_k. For each DT π_m define the variable z_m, the volume fraction of the DT-pyramid intersection. Then, for each DT π_m in $\{\pi\}$,
   a. Check if the central atom $A_i \in \pi_m$. If so, then set the volume fraction w_m to be the intersecting volume fraction z_m, and go on to (c). This is the case rendered in Fig. 5. If not, go on to (b).
   b. Further subdivide the subpyramid into parts intersected by other DTs, starting at the base, as outlined in the Section 4 and seen in Fig. 6. Add the pertinent volume fractions to z_m. It is possible that new DTs will be detected that are not found in $\{\pi\}$, i.e., DTs which intersect the pyramid, but do not intersect the Voronoi face. These new DTs are then added to $\{\pi\}$.
   c. Check that $\sum z_m = \Omega_k$. Add the volume intersecting the pyramid z_m to k_{im}, the volume fraction intersecting the Voronoi polyhedra.
9. Add the DTs in $\{\pi\}$ to the "master" DT list $\{K\}$ (if they are not already in $\{K\}$).

D. Check that $\sum_n k_{in} = Q_i$, where Q_i is the inputted volume fraction of the Voronoi polyhedron of atom i. Calculate the atomic deformation gradient $\mathbf{F}_i = \sum_n k_{in} \mathbf{F}_n$.

III. Finally, check that the atomic displacement gradient is conserved for the system by $\sum \mathbf{F}_i Q_i = \mathbf{F}_{\text{system}}$, and that the volume for all DTs is conserved, i.e., for all T_j in $\{T\}$ that $\sum_i z_{ij} = \phi_j$.

6. AN APPLICATION

This algorithm was used to study the change in structure of a static, atomistic model of polypropylene, developed by Theodorou and Suter [6]. The polymer is modelled as a single chain of atoms, with fixed bond lengths and bond angles, packed into a periodic parallelepiped, initially an 18.15 Å cube (total number of atoms = 455, degree of polymerization = 76, temperature = 233 K, density = 0.892 g/cm^3). Molecular movement can occur only by rotation around the skeletal C–C bonds. The van der Waals interaction between not directly bonded atoms is modelled by the Lennard-Jones potential energy function; backbone skeletal rotation is associated with a threefold rotational potential energy barrier. The methyl groups are lumped together into a single quasi-atom of appropriate size and potential parameters; the other hydrogen and carbon atoms are treated explicitly. The initial guess structure is grown by a Monte Carlo generation of a chain using the rotational isomeric state (RIS) theory, modified to account for long-range atomic interactions; the total energy of the system as a function of the bond rotation angles is then minimized using analytical derivatives. Figure 8 shows such an equilibrated structure; the skeletal carbon–carbon bonds are striped to emphasize the chain backbone.

Starting with a structure that is at a minimum energy, a small strain step is imposed on the periodic box continuation edges, which changes the position of the atoms in the parent chain with respect to the positions of the atoms in the image chains. Re-minimizing the energy of the system causes the polymer to seek a new conformation: repeatedly straining the box and then minimizing the energy simulates large deformations, in small incremental steps. Since time does not enter into the description of the system the strain rate is undefined.

Pure shear strain increments were imposed on the periodic box of the structure seen in Fig. 8, and the energy of the system re-minimized. The imposed incremental strain tensor was

$$\varepsilon = \begin{bmatrix} 1.0 & 0.0 & 0.0 \\ 0.0 & -1.0 & 0.0 \\ 0.0 & 0.0 & 0.0 \end{bmatrix} \times 10^{-3}.$$

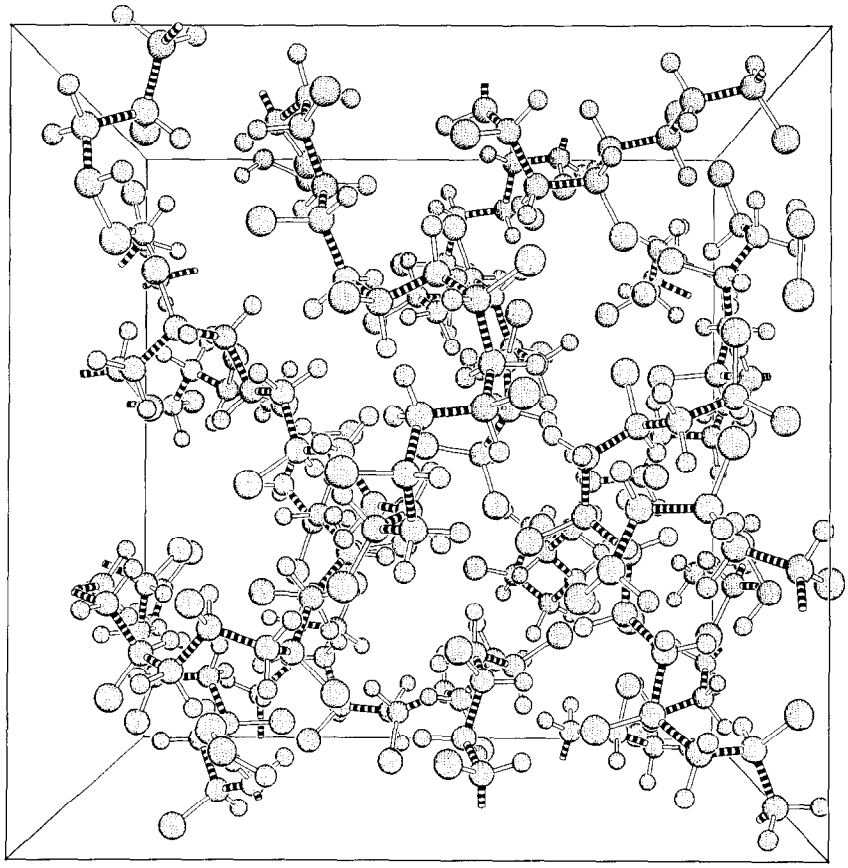

FIG. 8. Relaxed polypropylene structure. The backbone carbon–carbon bonds are shown striped. The large pendant atoms are "methyl" atoms, and the small pendant atoms are hydrogen atoms.

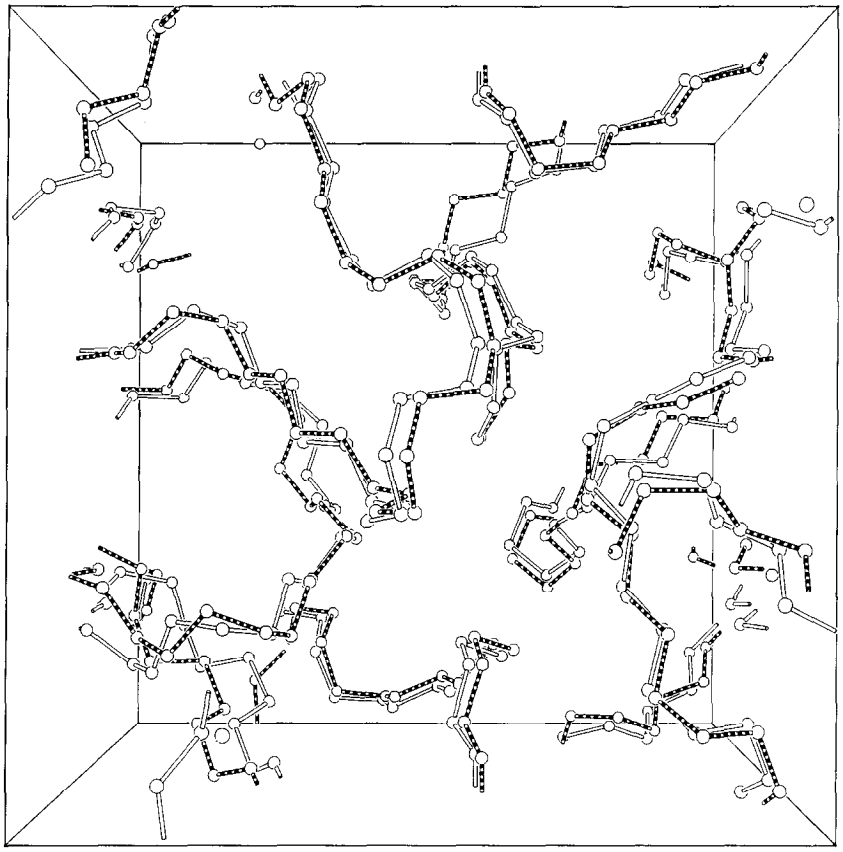

FIG. 9. Displacement of backbone chain. The original backbone is striped: it is the same structure as that drawn in Fig. 8. The backbone found after a strain increment was imposed on the system is shown with plain bonds.

While the deformation gradient imposed on the periodic box does not change the system volume, the algorithm presented here is not restricted to constant volume conditions. In Fig. 9 the backbone movement resulting from the imposed shear strain increment is demonstrated. The original backbone structure is shown with striped bonds (it is exactly the same structure that is shown in Fig. 8); the strained backbone is drawn unadorned. The "methyl" and hydrogen atoms have been removed for clarity. It is apparent that the whole chain moves in a complex way. Furthermore, it is impossible to distinguish a large movement of an atom from a large change of local environment because it is difficult to compare the displacement of a particular atom to the displacement of the neighbors of that atom.

To better understand the change in local structure, the atomic strain tensor for each atom was calculated, using the procedure presented above. Because the pendant hydrogen and "methyl" atoms were tied to the backbone with inextensible bonds at rigid angles, there can be no relative movement between the backbone and the pendant groups. Accordingly, we add the volume-weighted strains of the backbone carbon and pendant side groups together. This is the "effective segment unit" strain tensor, from which the scalar invariants in Eqs. (3) and (4) were found. Figure 10a illustrates the change in volume for each segment, plotted as circles of radius proportional to dilatation centered on the backbone carbon atoms (dashed circles indicate negative dilatation). In Fig. 10b the deviatoric distortion invariant is plotted. Three clusters of large distortion strains can be seen: in the center of the box, in the lower left-hand corner, and the lower right-hand side. Other regions, such the upper left-hand side, show relatively little distortion or dilatation, but can be seen to have large displacement in Fig. 9. The regions of large shear strains roughly coincide with the regions of large circles of dilatation. Figure 10 clearly improves perception of how the local environment has changed as a result of the imposed strain increment.

A detailed analysis of the change in the local atomic structure of this and other strain simulations will be published elsewhere as part of a comprehensive simulation of plastic deformation of glassy polymers at the molecular level.

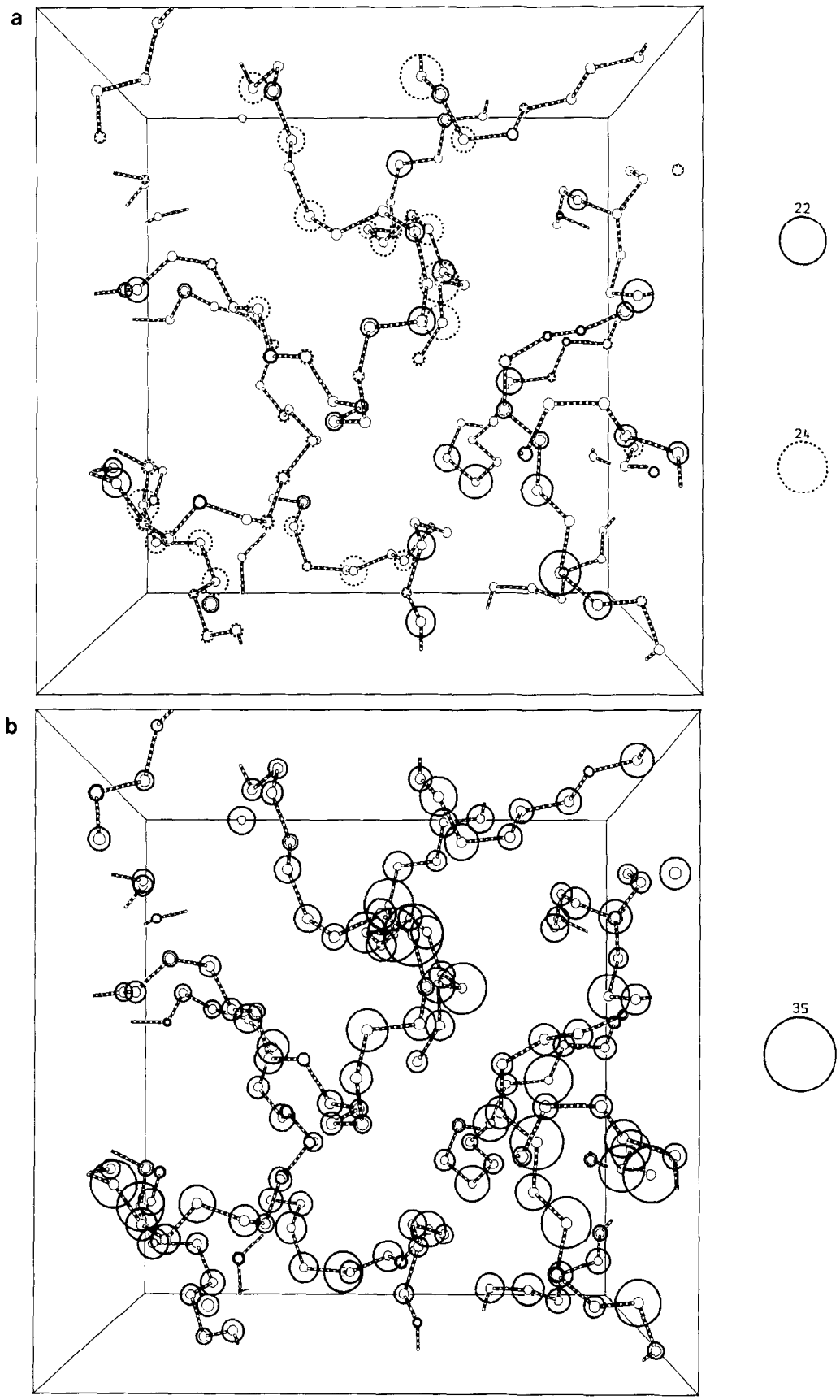

FIG. 10. (a) Dilatation of the effective segment unit, plotted as circles centered on the positions of the backbone carbon atoms. (b) Normal deviatoric distortion of the effective segment.

Note added in proof. The FORTRAN program of the algorithm described herein is available on written request.

ACKNOWLEDGMENTS

We gratefully acknowledge support from the Defense Advance Research Projects Agency, under ONR Contract N00014-86-K-0768. We thank Professor Masaharu Tanemura for providing the source code to their program that finds Voronoi polyhedra and acknowledge useful discussions with Professor David M. Parks.

REFERENCES

1. D. Deng, A. S. Argon, and S. Yip, *Phil. Trans. R. Soc. London A* **329**, 613 (1989).
2. J. H. R. Clarke and D. Brown, *Mol. Simul.* **3**, 27 (1989).
3. K. Maeda and S. Takeuchi, *Philos. Mag. A* **44**, 643 (1981).
4. D. Srolovitz, V. Vitek, and T. Egami, *Acta Metall.* **31**, 335 (1983).
5. M. Tanemura, T. Ogawa, and N. Ogita, *J. Comput. Phys.* **51**, 191 (1983).
6. D. N. Theodorou and U. W. Suter, *Macromolecules* **18**, 1467 (1985).